Journal of Cleaner Production 369 (2022) 133302

Contents lists available at ScienceDirect

Journal of Cleaner Production

journal homepage: www.elsevier.com/locate/jclepro

Spatio-temporal variation and dynamic scenario simulation of ecological risk in a typical artificial oasis in northwestern China

Qi Song [a], Bifeng Hu [b], Jie Peng [a,*], Hocine Bourennane [c], Asim Biswas [d], Thomas Opitz [e], Zhou Shi [f]

[a] College of Agriculture, Tarim University, Alar, 843300, China
[b] Department of Land Resource Management, School of Tourism and Urban Management, Jiangxi University of Finance and Economics, Nanchang, 330013, China
[c] URSOLS, INRAE, Orléans, 45075, France
[d] School of Environmental Sciences, University of Guelph, 50 Stone Road East, Guelph, ON, N1G 2W1, Canada
[e] INRAE, BioSp, Avignon, France
[f] Institute of Agricultural Remote Sensing and Information Technology Application, Zhejiang University, Hangzhou, 310029, China

ARTICLE INFO

Handling Editor: Jing Meng

Keywords:
Ecological risk assessment
Spatio-temporal variation
CA-Markov model
Scenario simulation

ABSTRACT

Landscape ecological risk assessments have played a critical role in measuring and predicting the quality and dynamic evolution of the ecological environment. In this study, a typical artificial oasis in the Alar reclamation area of Northwest China was selected as the research area. We acquired Landsat images from the past 30 years for the study area. Based on these remote sensing images, continuous long-term series and multi-temporal syntheses were combined to classify and construct a landscape ecological risk index. Our results showed a clear downward trend in the overall ecological risk in the Alar reclamation area between 1990 and 2019. Through scenario simulation, we found that the ecological risk of the research area is predicted to decrease in 2025 and 2030 under the two scenarios of natural growth and strict government control. Compared to the natural growth scenario, the increased area of construction and cultivated land is predicted to be less under the government control scenario, which contributes to the decrease in the overall ecological risk. Therefore, when formulating the overall plan for land use, the government should strictly control the increase in construction and cultivated land and prohibit illegal cultivation and blind reclamation of cultivated land. We used a classification method that is more suitable for the local study area, thereby increasing classification accuracy, and in turn, simulating and evaluating future landscape patterns more accurately. Our study provides a good reference for similar studies to be conducted in arid regions of northwest China and around the world.

1. Introduction

In recent decades, the ecological environment has deteriorated considerably in many regions due to human activity (Xu et al., 2019; Zhang et al., 2020; Hu et al., 2020a, 2022). Thus, ecological risk assessment is extremely important for the maintenance and protection of regional ecological security and has attracted widespread attention worldwide (Xu and Kang, 2017; Hou et al., 2020). Most recent studies have used remote sensing images from individual dates when analysing ecological risk (Ning et al., 2006; Yu et al., 2010; Li et al., 2018; He et al., 2019; Kabisch et al., 2019). In this study, we combined multi-temporal remote sensing images to assess the ecological risk profile of the Alar reclamation area and synthesised all available images from the same year to determine the maxima NDVI values. The synthesised images not only avoid errors that are caused by different plant growth conditions in different growth stages but can also eliminate the influence of cloud cover on the images. This could greatly improve the classification accuracy and provide more refined landscape pattern parameters for the construction of the landscape ecological risk.

In addition, the scale and pattern of the future ecological space directly affect the ecological security of the national space (Wang et al., 2020a). Therefore, it is of great theoretical and practical significance to construct a scientific and reasonable model that can simulate and predict the ecological space, thereby facilitating the protection of the ecological environment and optimal control of the national space (Jin et al., 2019; Fu et al., 2020). Changes in landscape patterns can be analysed and

* Corresponding author.
E-mail address: pjzky@163.com (J. Peng).

https://doi.org/10.1016/j.jclepro.2022.133302
Received 8 August 2021; Received in revised form 13 July 2022; Accepted 22 July 2022
Available online 4 August 2022

simulated using various models, of which the Cellular Automata (CA) model is widely used (Wang et al., 2020b; Mokarram et al., 2021; H. Wang et al., 2021). The CA–Markov model combines the ability of the CA model to simulate spatial changes of complex systems and the advantages of the Markov model for long-term prediction, which not only improves the prediction accuracy of land use type transformation but also effectively simulates the spatial changes in land use patterns (Rahman and Ferdous, 2021; Zhang et al., 2021a). The CA–Markov model is scientifically and practically sound and overcomes the shortcomings of traditional land evolution simulation models (Zhang et al., 2021b).

The study area is a typical artificial oasis. Artificial oases can assist humans to effectively prevent the extrusion and erosion of arid climate environments and maintain the stability and development of oasis systems (T.Y. Wang et al., 2021; Zheng et al., 2022). Currently, artificial oases are an important ecological haven for humans to avoid the negative effects of an arid climate. Thus, it is important to predict the potential ecological risks of the area in the future. However, as land use change is a continuous process, a lot of critical information may be missed in typical time-transect data. Furthermore, there are various crop types in the study area, with different phenological periods. For example, wheat is usually harvested in May and June, after which the farmland that was previously planted with wheat can be wrongly classified as bare land. Therefore, we used the maximum composite value of the multi-phase normalised difference vegetation index (NDVI) for classification based on images from different years, which could reduce the rate of misclassification. Although this method has been used in many areas, it has not been reported in the artificial oasis areas of Northwest China. The vegetation in the study area changes rapidly in all seasons of the year. Consequently, the maximum multi-phase NDVI composite value is highly suitable for application in the study area.

It can greatly improve the prediction accuracy in the area, as other methods are not suitable for this research area. To this end, we collected all the Landsat images that covered the study area over the past 30 years. Our study generated new data to address the research gap when compared to studies that use typical time-lapse as the basic data. Moreover, the combination of continuous long-term time series and multi-temporal NDVI maxima improved the accuracy of landscape classification, thereby rendering our landscape pattern information and prediction more accurate. Subsequently, we predicted future ecological risks and revealed the characteristics of the spatio-temporal changes in the ecological risks in the study area. Our results have significant implications for efforts pertaining to the protection of the stability and health of the ecosystem in the study area.

2. Materials and methods

2.1. Study area

The survey region in this study was located in the Alar reclamation area in the arid area of Northwest China, with a total area of 4105.92 km^2 (40° 22′ 0″–40° 57′0″ N, 80° 30′ 0″–81° 58′ 0″ E; Fig. 1a). It is adjacent to the Taklamakan Desert and belongs to the Tarim Basin, with the Tianshan Mountains to the north and the Kunlun Mountains to the south, creating a spatial pattern of mountains surrounding the basin and a desert surrounding the oasis. The study area is a typical arid area of an artificial oasis and features low rainfall, serious soil salinisation, and a lack of water resources. The Alar reclamation area was an inaccessible wasteland for an extended period of time. Since the 1950s more than 80,000 ha have been reclaimed as agricultural land. In 2019, the GDP and total agricultural output of the Alar reclamation area were 30.95 and 27.186 billion yuan, respectively (Peng et al., 2019; Cao et al., 2022;

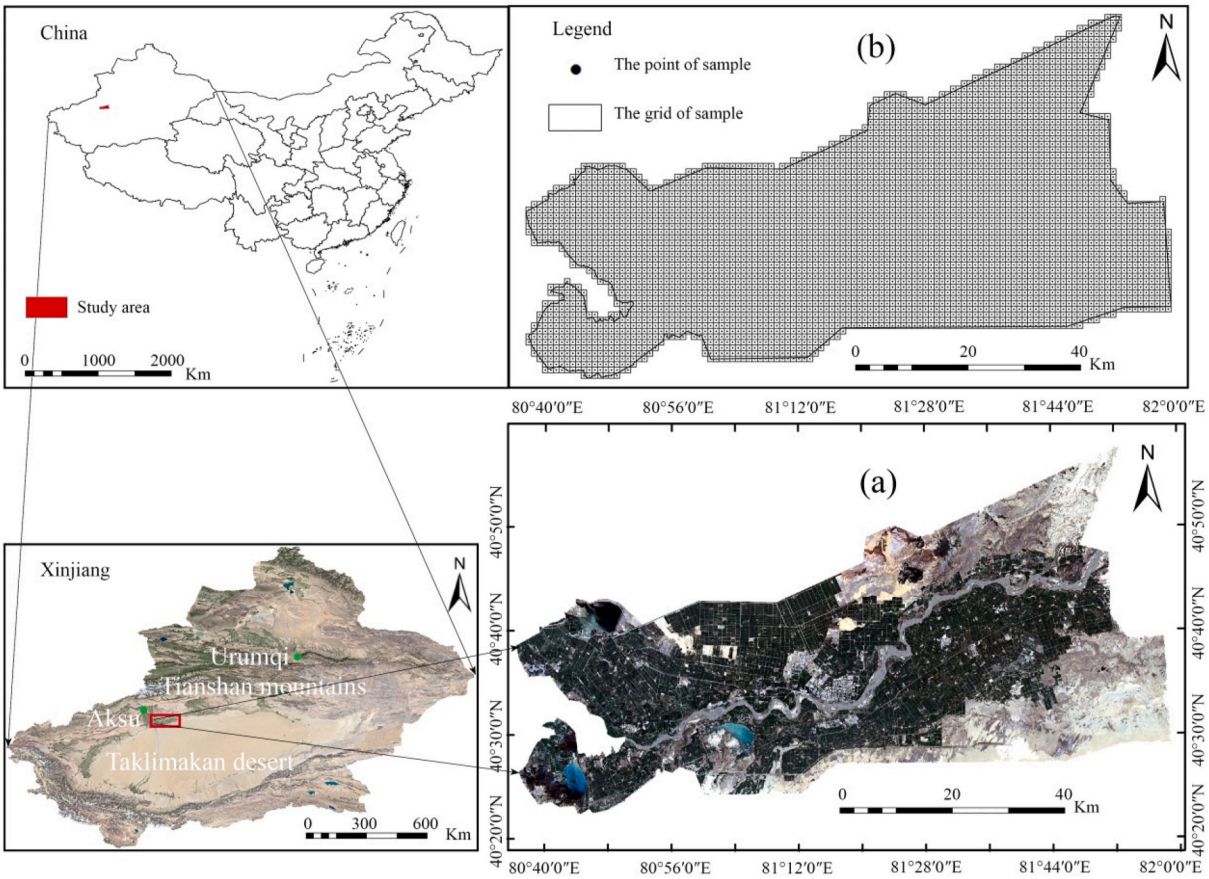

Fig. 1. (a) Location of the study area and (b) ecological risk assessment units on a simple map of the Alar reclamation area.

Lv et al., 2022; Wang et al., 2022; Zhang et al., 2022).

2.2. Data acquisition and pre-processing

2.2.1. Data acquisition

The remote sensing data were downloaded from the website https://earthexplorer.usgs.gov/. The downloaded images had orbital numbers of 146–32 and a spatial resolution of 30 m, with cloud cover of less than 40% (multi-temporal image synthesis can eliminate the influence of cloud cover). Since the Landsat series of the sensors had been continuously updated over the past 30 years, the following sensors were selected for the remote sensing images in this study: Landsat 5 from 1990 to 1998, Landsat 7 from 1999 to 2012, and Landsat 8 from 2013 to 2019. We collected the past 30 years' worth of Landsat Thematic Mapper remote sensing images, which cover the study area. The cloud coverage of each scene and the number of images in each year are shown in Fig. 2.

2.2.2. Normalised difference vegetation index synthesis of remote sensing images and landscape classification

A pre-process was employed for the Landsat images from 1990 to 2019 using the ENVI software. This included radiometric calibration, atmospheric correction, geometric correction, cropping, image enhancement, and band calculation. The NDVI was then calculated for each view image. Afterwards, we synthesised the maximum value of all the NDVIs in the same year to obtain a map showcasing the maximum NDVI composite for each year. We used the eCognition software for object-oriented classification of the landscape. The landscapes were divided into six types: cultivated land, forest and grassland, garden land, water body, construction land, and unused land. The processing flow of the remote sensing images is presented in Fig. 3.

2.3. Landscape ecological risk index

2.3.1. Dividing the area into ecological risk zones

Considering the spatial heterogeneity, patch size, area of the survey region, and sampling density (Ni et al., 2019; Yuan et al., 2019), a 1 km × 1 km square grid was constructed and used to conduct evenly spaced sampling fishing nets in the Alar reclamation area using ArcGIS software. The Alar reclamation area was divided into 4337 ecological risk communities, as shown in Fig. 1b.

2.3.2. Construction of the landscape ecological risk index

The landscape ecological risk index (*ERI*) can provide relevant information on landscape patterns and can be used to evaluate the regional ecological risk (Liang et al., 2019). The survey region in this study is a typical artificial oasis area; thus, the landscape is strongly affected by human activities, and this makes the ecosystem more fragile. The landscape fragmentation index (C_i), landscape separation index (S_i), and landscape dominance index (D_i) were selected and combined to construct the landscape disturbance index (LDI_i) model (Ma et al., 2019). Meanwhile, using the LDI_i and landscape fragility index (LFI_i) were used to construct the landscape *ERI*. The correlation between cultivated land and human activity in the artificial oasis area was the largest, and the fragility and sensitivity coefficients were the highest (Wang et al., 2020a; Zhang et al., 2020). Thus, in this study, the fragility coefficients of unused and cultivated land were assigned values of 5 and 6, respectively. The specific calculation formulas are shown in Table 1, through which we could link the landscape index and landscape ecological risk to determine the change in the landscape ecological risk in the study area.

2.4. Spatial-temporal analysis method of landscape ecological risk

The geostatistical method has been widely used to monitor, model, and estimate the spatial correlation and spatial patterns of target variables (Webster and Oliver, 2008; Zhang et al., 2016; Shi et al., 2019; Xia et al., 2019; Hu et al., 2020b). The experimental variogram is used to explore the spatial structure of the variables (Webster and Oliver, 2008; Xia et al., 2020). Its calculation formula is as follows:

$$\gamma(h) = \frac{1}{2n(h)} \sum_{i=1}^{n(h)} [Z(x_i + h) - Z(x_i)]^2$$

where $\gamma(h)$ is the variogram; $n(h)$ is the number of the pairs of sample points with a distance of h; Z is the random variable of a certain system attribute; $Z(x_i)$ and $Z(x_i + h)$ are the values taken at the points of the variables x_i and $(x_i + h)$, respectively.

The geostatistics software GS+ was used to achieve optimal fitting of the experimental semi-variogram model, based on which the ordinary kriging interpolation was employed (Hu et al., 2020a; Li et al., 2020a) in the ArcGIS software. The natural breakpoint method was used to classify the study area into five classes (extremely low-risk, low-risk, medium-risk, high-risk, and extremely high-risk) based on the ecological risk map of each year. Subsequently, we used a spatial overlay analysis for quantitatively assessing the transformed direction and area of regions with different ecological risk levels.

2.5. Spatial autocorrelation analysis

Spatial autocorrelation analysis examines whether the values of the

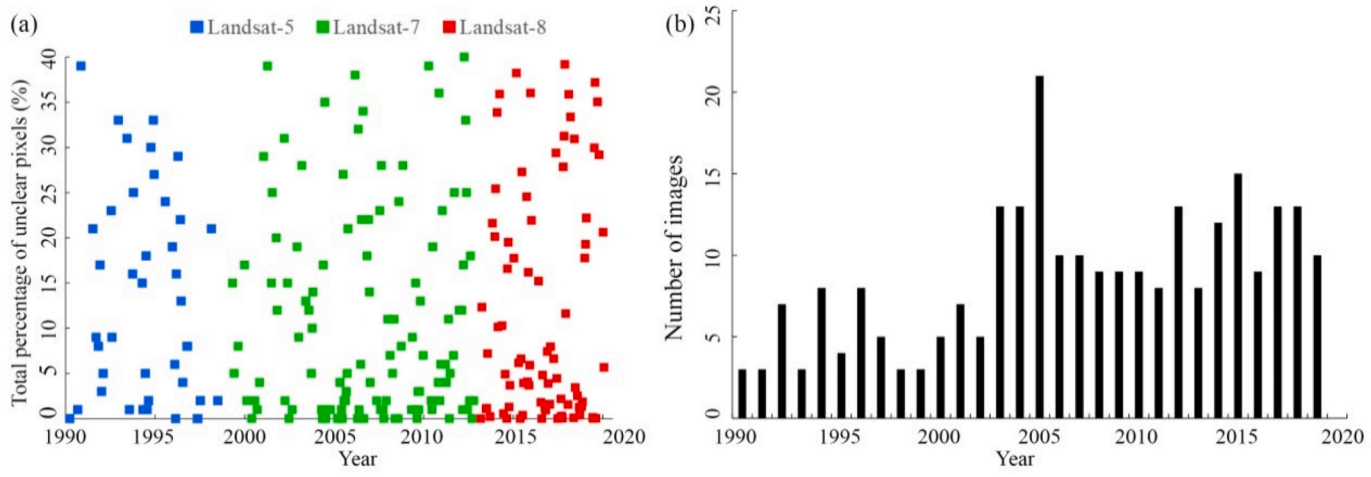

Fig. 2. Remote sensing data. (a) The percentage of cloud cover in each view image; (b) the number of images per year.

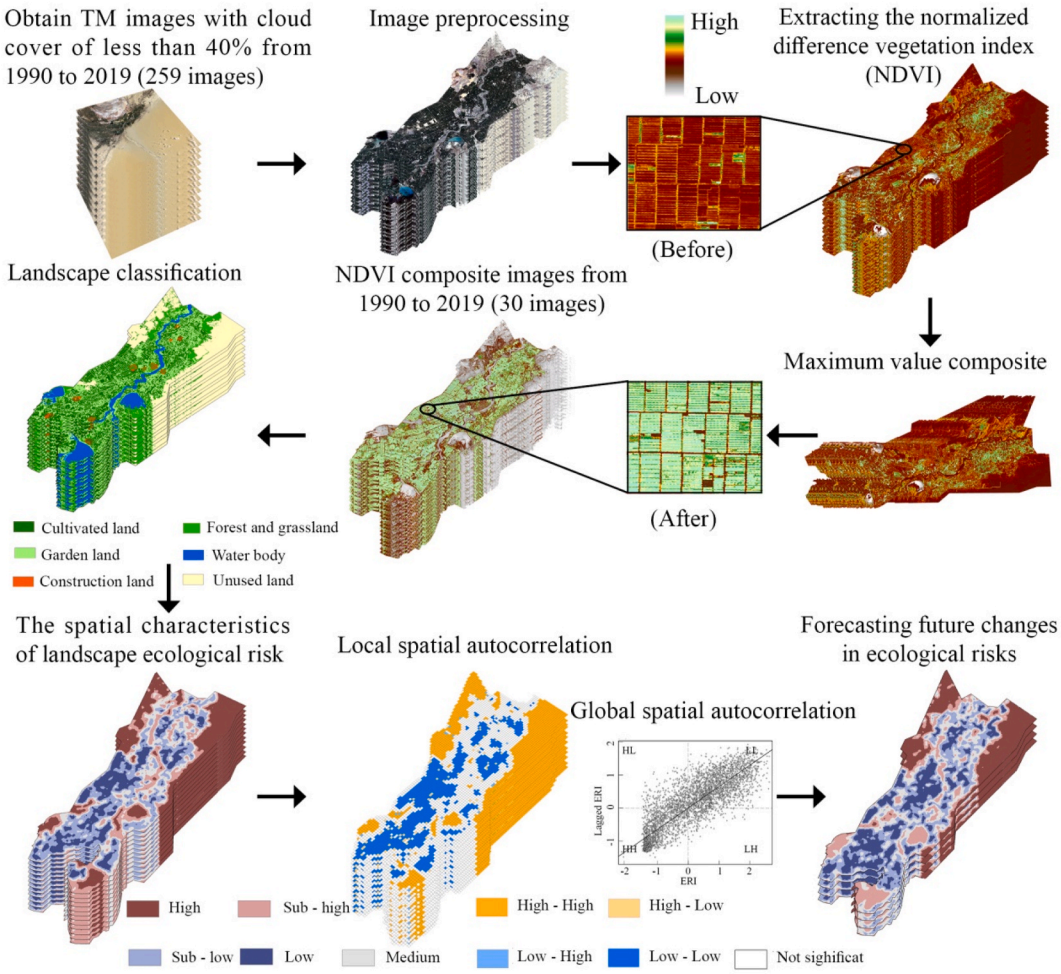

Fig. 3. Framework of this study.

Table 1
Formulas for calculating the ecological risk index.

Landscape	Ecological meaning	Formula	Formula description
Landscape fragmentation index	The degree of patch fragmentation in each landscape type	$C_i = n_i / A_i$	n_i is the patch number of landscape i; A_i is the total area of landscape i (Peng et al., 2014; Xie et al., 2020)
Landscape separation index	The degree of patch separation in each landscape type	$S_i = A / 2A_i \cdot \sqrt{n_i / A}$	A is the total area of the entire landscape
Landscape dominance index	The degree of patch importance in each landscape type	$D_i = 0.25\left(\frac{n_i}{N} + \frac{m_i}{M}\right) + 0.5\left(\frac{A_i}{2A}\right)$	N is the total number of patches; m_i is the sample number of patch i; M is the total number of samples
Landscape disturbance index	The degree of external interference in different landscape types	$LDI_i = aC_i + bS_i + cD_i$	a, b, and c are weights of indices C_i, S_i, and D_i, respectively. $a = 0.5$, $b = 0.3$, $c = 0.2$
Landscape fragility index	The resistance ability of the external interference in different landscape types	LFI_i obtained by artificial assignment and normalization	Modified in this study according to the specific research area status based on the value presented in previous studies (Jin et al., 2019; Li et al., 2020). Cultivated land = 6, Unused land = 5, Forest and grassland = 4, Water body = 3, Garden land = 2, and Construction land = 1
Ecological risk index	The relative sizes of integrated ecological losses in a specifically selected sample	$ERI = \sum_{i}^{N} \frac{S_{ki}}{S_k} LDI_i \cdot LFI_i$	N is the number of landscape types in the sample areas; S_{ki} is the area of landscape type i in the sample k; S_k is the area of sample k

target variable at the spatial location are correlated with neighbouring points, and it is divided into global spatial autocorrelation and local spatial autocorrelation (Hu et al., 2017, 2019; Cui et al., 2018). In this study, Moran's I index values were calculated using GeoDa software to assess the degree of spatial autocorrelation of the target variables. Using the Moran's I index, we could detect whether there were statistically significant relationships in the ecological risks in local areas (Shi et al., 2018; Hu et al., 2020b). The hot spots indicate regions with high-value ecological risk clusters, whereas the cold spots represent regions with low-value ecological risk clusters.

2.6. Prediction of the ecological risk based on the Cellular Automata–Markov model

The CA model is a discontinuous spatiotemporal dynamic model, which is characterised by discrete temporal and spatial states (Rahnama, 2020; Sww et al., 2020). The Markov method is a special stochastic process based on the stochastic process theory that was proposed by the mathematician Markoff. By calculating the initial probability of different states and the relationship between the transition probabilities, the changing trend in the landscape pattern over time was determined and the change in the landscape pattern was predicted. In the raster map of the landscape type, each pixel is a cell, and the landscape type of each cell is the state of the cell. The transition of the cell state is determined using the conversion area matrix and the conditional probability image for simulating the changes in the landscape patterns (Ghosh et al., 2017; Ama and Hw, 2020).

We forecasted the future ecological risks to reveal the spatio-temporal variation and related drivers of ecological risks in the study area, which is expected to provide implications for the construction of ecological civilization and achieving sustainable development in the study area. In the plan issued by the Xinjiang Province, the aim is to build a demonstration area of ecological civilization in arid areas by the year 2025. Meanwhile, in the National Land Planning Outline issued by the Chinese government, several critical goals are set, such as realizing a safe and harmonious ecological environment protection pattern and strengthening natural ecological protection, especially in ecologically fragile areas like Xinjiang Province (http://www.gov.cn/gongbao/content/2017/content_5171326.htm). To serve these strategic objectives, we predicted the ecological risk in the study area in 2025 and 2030 (http://www.xinjiang.gov.cn/xinjiang/fgwjx/202202/81d6eb8056104b2c992f3fbcda67ac58.shtml). Information on the landscape types in the study area was extracted for 30 periods from 1990 to 2019 and the CA–Markov model was used to simulate and predict the direction of landscape pattern development in 2025 and 2030 under the natural growth and government control scenarios in the Alar reclamation area.

To improve the prediction accuracy of the ecological risk, we collected information on 15 potential influencing factors including elevation, slope, aspect, distance from highways, railways, highways and water systems, temperature, precipitation, population, gross domestic product, social fixed asset investment, primary industry, gross agricultural production and cotton prices, and landscape classification data. We used the CA–Markov model in the IDRISI software to simulate the future landscape pattern of the study area. Thereafter, we first predicted the ecological risk of the study area in 2019 based on the 21 periods of the landscape classification data from 1990 to 2010 and the 15 potential influencing factors. Then, the prediction result for 2019 was compared with the real ecological risk of 2019, which was used to validate the performance of our CA–Markov model. Finally, we predicted the ecological risk of the survey region in 2025 and 2030 using the CA–Markov model that we developed.

3. Results

3.1. Changes in the ecological risk index of the landscape

Our results show that from 1990 to 2019, the landscape fragmentation indices (C_i) of cultivated land and construction land were relatively high with a decreasing trend. Meanwhile, the C_i values of the water body and unused land were close to 0, which indicates that their spatial distributions are very concentrated (Fig. 4). The landscape separation indices (S_i) of construction land and cultivated land exhibited a decreasing trend and the spatial distribution characteristics changed from random distribution to concentrated distribution. The landscape dominance index (D_i) of unused land showed a downward trend, and the degree of interference gradually increased. Additionally, the D_i value of cultivated land showed an upward trend. Due to the increase in demand

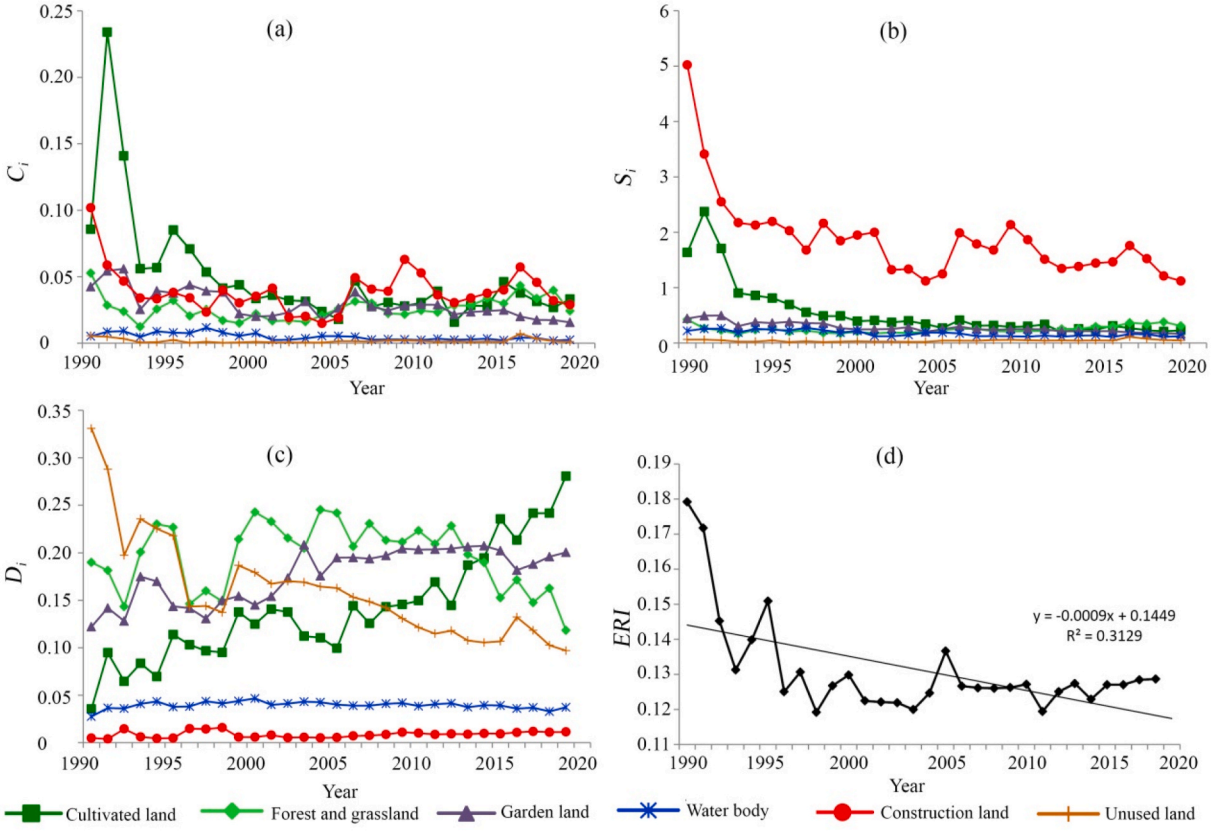

Fig. 4. Landscape pattern metrics from 1990 to 2019.

for cultivated land, large areas of wasteland have been reclaimed, increasing the D_i value of the cultivated land. As shown in Fig. 4 (d), the *ERI* of the Alar reclamation area decreased from 0.1791 in 1990 to 0.1286 in 2019, indicating that the ecological risk of the study area has decreased over the past 30 years.

The transformation matrix of land use types in the Alar reclamation area from 1990 to 2019 is presented in Table 2. From 1990 to 2019, the cultivated land area increased by 1516.19 km^2 with the transformation predominantly from unused land. Forest and grassland areas decreased by 39.63 km^2. The extent of the developed area increased by 37.82 km^2 with the transformation being predominant in cultivated land (see Table 2).

3.2. Spatio-temporal variation in the landscape ecological risk

3.2.1. Semi-variogram analysis

We determined the change in ecological risk during 30 periods from 1990 to 2019. However, to be concise, we only present the changes in the landscape ecological risk for four typical time intervals in 1990, 2000, 2010, and 2019. The optimal fitting of the theoretical model of the variance function was performed using the sampling data of 4337 ecological risk communities for each year and the relevant variance functions and parameters are presented in Table 3. In 1990 and 2019, the exponential model was fitted, while in 2000 and 2010, the spherical model was more suitable.

The sill value decreased from 0.0027 in 1990 to 0.0014 in 2000 and then increased to 0.0024 in 2019, indicating that the uneven spatial distribution of the landscape ecological risk intensity decreased first and then increased between 1990 and 2019. The range value increased from 6900 m in 1990 to 27,600 m in 2019, indicating that the relevant range of the ERI is gradually expanding. The nugget/sill value of the ERI decreased first and then increased, ranging from 0.641 to 0.846. This indicates that the spatial correlation of the ecological risk value decreased first and then increased.

3.2.2. Spatial characteristics of the landscape ecological risk

The spatial distribution of the landscape ERI and the proportions of each risk level in the Alar reclamation area in 1990, 2000, 2010, and 2019 are shown in Fig. 5. As shown in Fig. 5, in 1990 the ecological risk was high in most areas of the survey area, while areas with a low value were mainly distributed along the Tarim River. The main landscape type in 1990 was unused land and the ecological environment was very fragile; therefore, the ecological risk level was high. In 2000, the area that was occupied by low-risk areas expanded, while the areas with high ecological risk decreased. A large reservoir is present in the southwestern corner of the study area. It is evident from the remote sensing images that a large area of wasteland in the southwestern corner was transformed into wetlands in 1999, where vegetation was planted to maintain the ecological balance around the reservoir. This led to localised changes in ecological risks. Then, in 2010, the ecological risk in the northwestern part of the Alar reclamation area changed from a high level to a medium level. This could mainly be attributed to the fact that this region was reclaimed and expanded, which led to increased planting density, ecosystem stability, and reduced ecological risks. By 2019, the proportion of areas with very low ecological risk and low ecological risk had increased. Most parts of the survey region had low or medium ecological risks. Areas with high ecological risk were mainly located in the southeastern and northeastern parts of the study area.

3.2.3. Spatial characteristics of the dynamic changes in the landscape ecological risk

As presented in Fig. 6, the areas of reduced ecological risk levels between 1990 and 2000 were concentrated along the Tarim River. Regions with an increased ecological risk level were mainly distributed in the northern and southern parts of the Alar reclamation area. From 2000 to 2010, the change in the ecological risk was more complex and irregular in the Alar reclamation area. Notably, large areas in the eastern part of the survey region showed a decreased ecological risk level. This was due to extensive reclamation of unused land in this region. Also, an increase in the cultivated land reduced the ecological risk. From 2010 to 2019, the areas of reduced ecological risk were mainly located along the Tarim River. The expansion of the arable area showed a tendency to spread outwards from the Tarim River.

Overall, the ecological risk level showed a decreasing trend in the survey region between 1990 and 2019. The areas with altered ecological risk levels were mainly located along the Tarim River and in the northwestern part of the Alar reclamation area. This is because these areas are close to the water source and conducive to agriculture. With the development of agriculture, the planting structure in this area has become more diversified and the ecosystem is more stable, which increases the ability of the area to resist external interference. Therefore, the degree of dominance increased, reducing the ecological risk level. However, most of the unused land around the reclamation area is abandoned land with a high degree of salinisation. The ecological structure is fragile and easily affected by anthropogenic actions. Thus, the ecological risk of the central part of the reclamation area was lower than that of the unused land around the reclamation area.

3.3. Spatial autocorrelation analysis

3.3.1. Global spatial autocorrelation

As shown in Fig. 7, the global Moran's I values of the ERI in 1990, 2000, 2010, and 2019 were 0.317, 0.625, 0.716, and 0.692, respectively. All four values are positive and show an increasing trend, indicating a clear positive spatial correlation for the ERI in the Alar reclamation area. Thus, the spatial relevance of the ecological risks within the study area was strengthened.

3.3.2. Local spatial autocorrelation

The spatial autocorrelation is not only used for the clustering of land uses but is also used for the analysis of regional management and landscape patterns (Peng et al., 2020a, 2020b). The global spatial autocorrelation can only reveal the spatial autocorrelation in the whole study area. Therefore, in this study, the local Moran's I index was also calculated to analyse the local spatial clustering of areas with high or low ecological risks. Maps of local autocorrelation of the ecological risks

Table 2
Transformation matrix (km^2) of land use types in the Alar reclamation area from 1990 to 2019.

2019								Total
		Cultivated land	Forest and grassland	Garden land	Water body	Construction land	Unused land	
1990	Cultivated land	–	0.38	349.64	2.86	16.11	0.00	368.99
	Forest and Grassland	14.09	–	8.81	6.77	8.60	1.36	39.63
	Garden land	832.59	0.36	–	15.84	11.59	0.00	860.38
	Water body	4.94	0.58	15.69	–	0.04	0.00	21.25
	Construction land	0.00	0.00	0.00	0.00	–	1.28	1.28
	Unused land	664.57	4.64	1160.44	103.36	1.48	–	1934.48
Total		1516.19	5.96	1534.58	128.83	37.82	2.64	

Table 3
Parameters of the theoretical model of the variogram.

Year	Model	Nugget	Sill	Range (m)	Nugget/Sill	R^2	RSS ($\times 10^{-10}$)
1990	Exponential	0.000416	0.002702	6900	0.846	0.635	2608
2000	Spherical	0.000522	0.001454	15,000	0.641	0.753	1664
2010	Spherical	0.000484	0.001538	17,800	0.685	0.931	596.6
2019	Exponential	0.00066	0.002380	27,600	0.723	0.943	1184

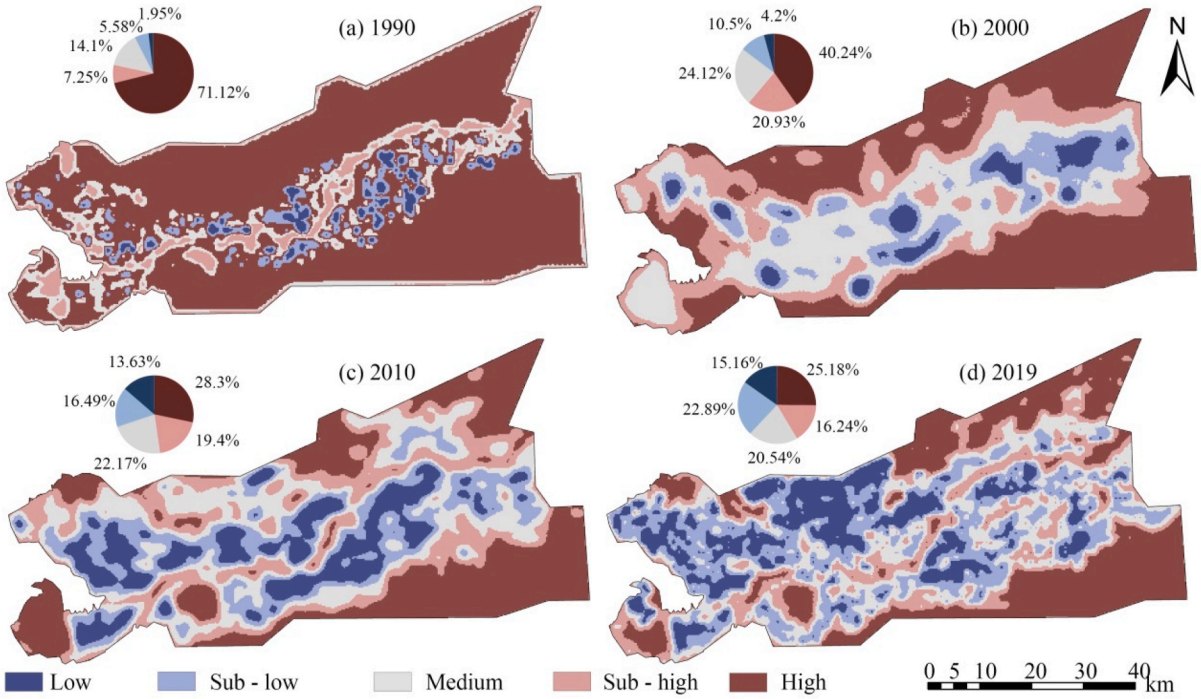

Fig. 5. Spatial pattern and proportion of the area in each ecological risk index class in 1990, 2000, 2010, and 2019.

in the study area in 1990, 2000, 2010, and 2019 are provided in Fig. 8. The areas with high-high clusters of ecological risk significantly decreased between 1990 and 2019. The regions with clusters of high-high ecological risk showed a shrinking spatial trend from the outside to the inside of the survey region. The main landscape type in the regions with clusters of high-high ecological risk was unused land with low vegetation coverage and a single vegetation structure. Thus, the ecological environment is fragile in these areas. In contrast, areas with clusters of low-low ecological risk expanded in the areas in the central part of the survey region when compared to the outside. These regions featured a low ecological risk. The main landscape types in these regions were cultivated land, garden land, and construction land with relatively stable ecosystems.

3.4. Forecasting future changes in the ecological risks

The success of the CA-Markov model for simulating landscape patterns lies in the determination of land suitability and the land use transfer probability matrix. This study used the CA module to generate an atlas of land use suitability. Then, we integrated the land use transfer probability matrix that was generated by using the Markov model, information on the 15 influencing factors, and landscape classification maps from 1990 to 2010 to simulate the landscape patterns of the reclamation area in the study area in 2019. Thereafter, we evaluated the ecological risk based on the simulated results and compared it to the actual ecological risks in the study area to assess its accuracy.

The accuracy of the 2019 post-simulation results was further evaluated by using the confusion matrix (Table 4). As shown in Table 4, the deviations in the simulation accuracy were mainly induced by the new industrial parks that were built under the urban planning policy in 2005, which increased the area of construction land, resulting in lower accuracy for parkland and construction land. However, the overall classification accuracy of the Alar reclamation was 90.27% and the Kappa coefficient was 0.8693, indicating that the CA–Markov model can be used to simulate land use changes in the Alar reclamation area, develop scenario simulations, and forecast ecological risks for 2025 and 2030.

Next, the land use layout map for 1990 in the Alar reclamation area was used as the initial bench map, and the CA–Markov module in the IDRISI software was used to input the suitability atlas of each class and combined with the land use change transfer probability matrix. The number of simulation cycles was set at 7. Fig. 9 shows the distribution of the landscape patterns in the study area for 1990, 2000, 2010, 2019, 2025, and 2030. Using the same methods, projections for the short-term periods for 2025 and 2030 were achieved using the landscape classification data from 1990 to 2019.

The ecological risk was simulated and predicted for 2025 and 2030 under natural growth and government control, respectively (Fig. 10). The scenario of natural growth assumes maintenance of the existing vegetation, whereas the scenario of strict government control assumes that the government takes strict measures to reduce the conversion rate of construction land and removes the permanent basic farmland boundary. Under the scenario of strict government control, the conversion rate of cultivated land decreased from 50 to 30%.

As revealed by the simulation results, in 2025, the overall ecological risk of the study area under the government control scenario (Fig. 10a) is predicted to be lower than that under the natural growth scenario

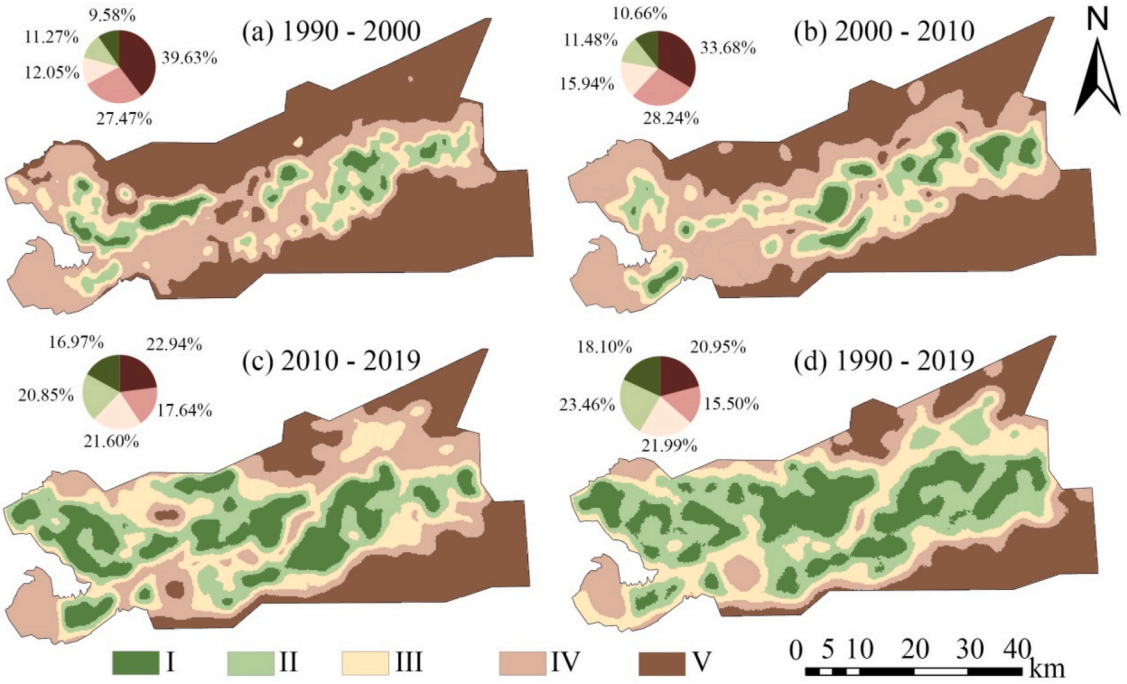

Fig. 6. Spatial distribution of the change in the ecological risk classes and change in the proportion of the area in each class in the Alar reclamation area during (a) 1990–2000, (b) 2000–2010, (c) 2010–2019, and (d) 1990–2019. Classifications: I, zone of extreme ecological improvement; II, zone of ecological improvement; III, zone of ecological stability; IV, zone of ecological deterioration; and V, zone of extreme ecological deterioration.

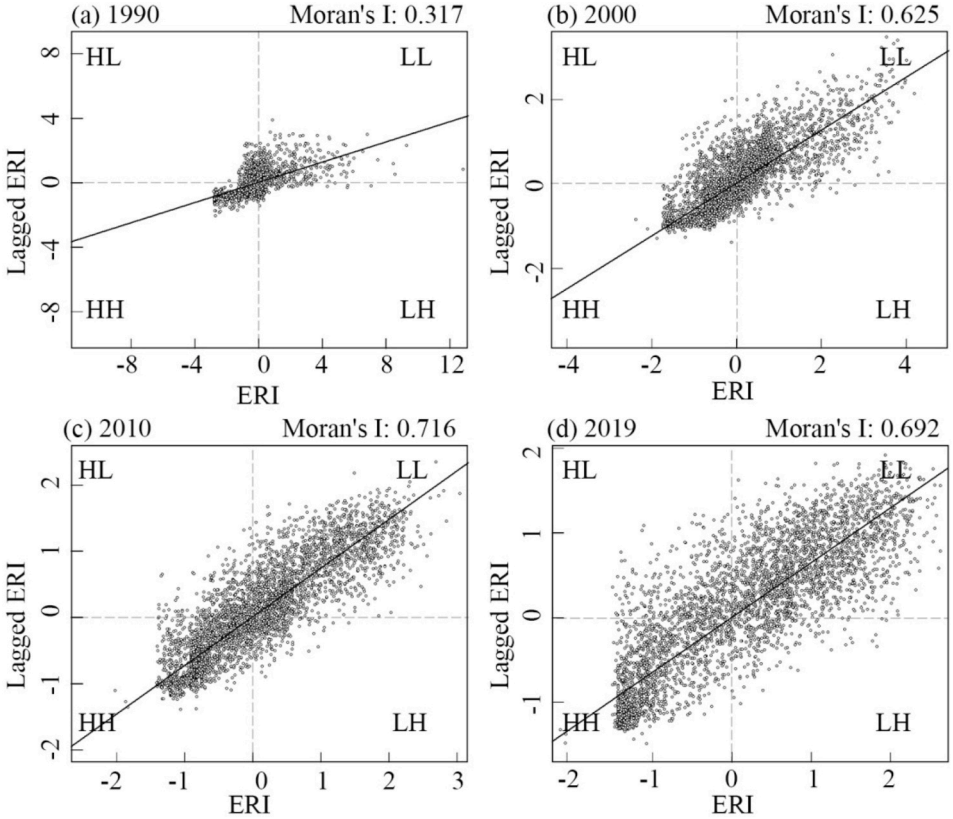

Fig. 7. Global Moran's I scatter figures of the landscape ecological risk index (ERI) in the Alar reclamation area for (a) 1990, (b) 2000, (c) 2010, and (d) 2019. HL, High - Low; HH, High - High; LL, Low - Low; LH, Low - High.

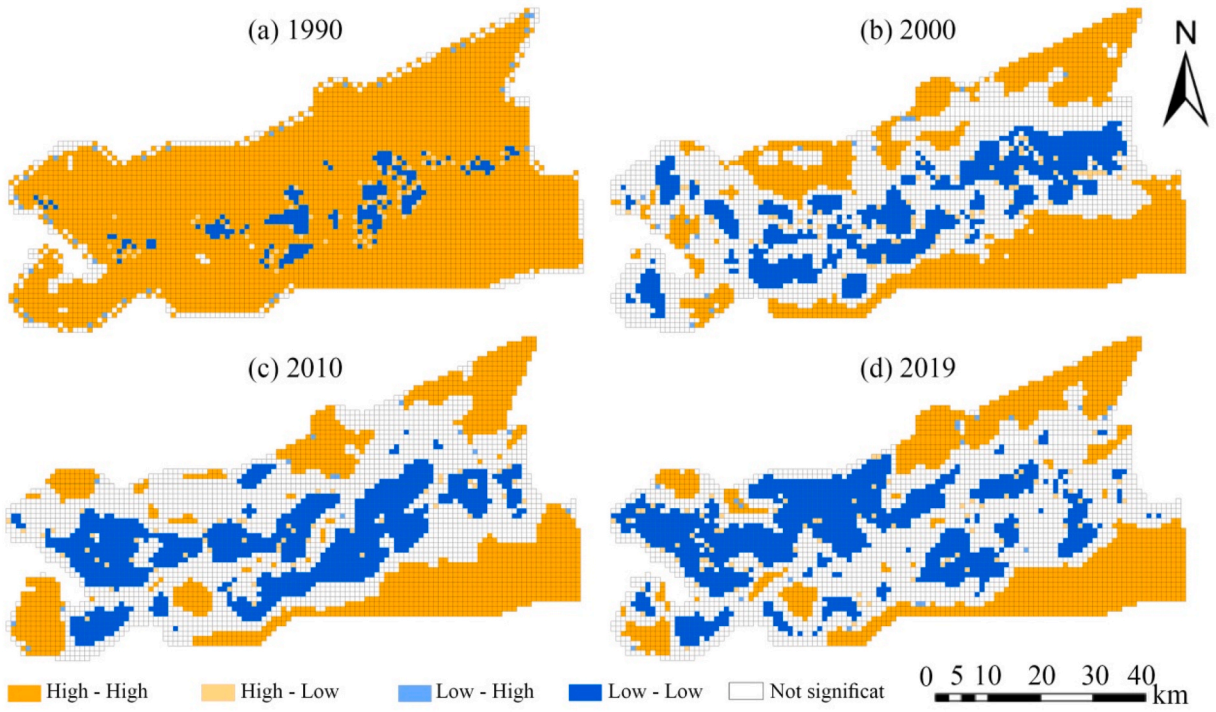

Fig. 8. Local spatial autocorrelation of the landscape ecological risks in (a) 1990, (b) 2000, (c) 2010, and (d) 2019 in the Alar reclamation area.

Table 4
Accuracy evaluation of the land use simulation in the Alar reclamation area in 2019.

Predicted class								Total	UA (%)
		Cultivated land	Forest and grassland	Garden land	Water body	Construction land	Unused land		
Real class	Cultivated land	**80,470**	3721	951	581	438	7008	93,169	**86.37**
	Forest and Grassland	762	**91,120**	237	2617	67	2943	97,746	**93.22**
	Garden land	10,452	2241	**29,986**	628	57	5435	48,799	**61.45**
	Water body	0	2003	54	**78,852**	0	2698	83,607	**94.31**
	Construction land	0	0	33	5	**9656**	633	10,327	**93.50**
	Unused land	0	10,378	0	75	0	**210,814**	221,267	**95.28**
Total		91,684	109,463	31,261	82,758	10,218	229,531		
PA (%)		**87.77**	**83.24**	**95.92**	**95.28**	**94.50**	**91.85**	**OA%**	**90.27**

Diagonal values in bold are the number of correctly classified pixels for each category; vertical bold values are the user accuracy (UA) for each category; horizontal bold values are the cartographic accuracy (PA) for each category. OA, overall accuracy.

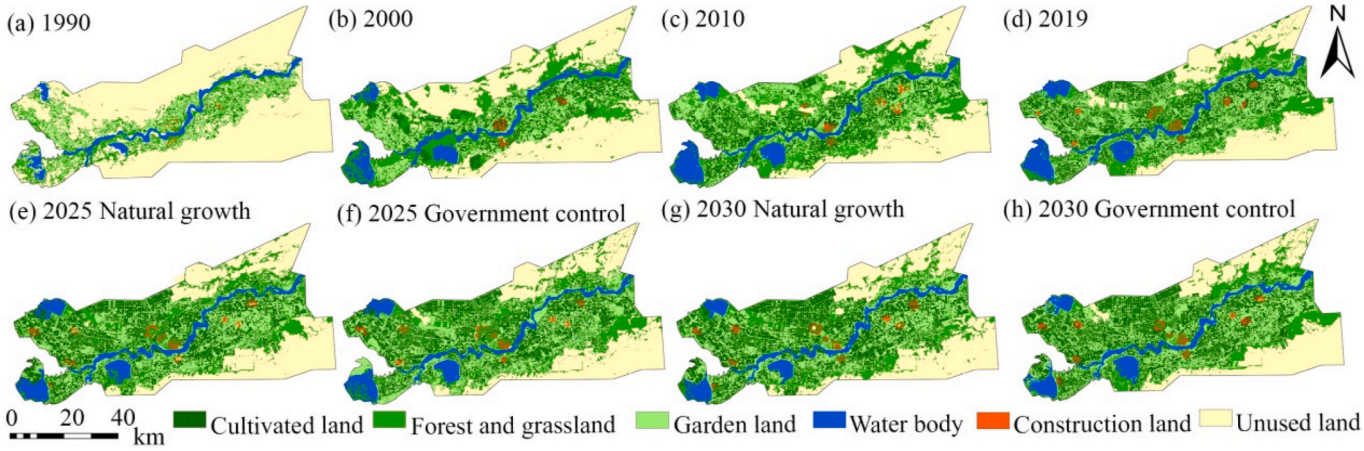

Fig. 9. Distribution of the landscape patterns in (a) 1990, (b) 2000, (c) 2010, (d) 2019, (e) 2025 under natural growth, (f) 2025 under government control, (g) 2030 under natural growth, and (h) 2030 under government control in the Alar reclamation area.

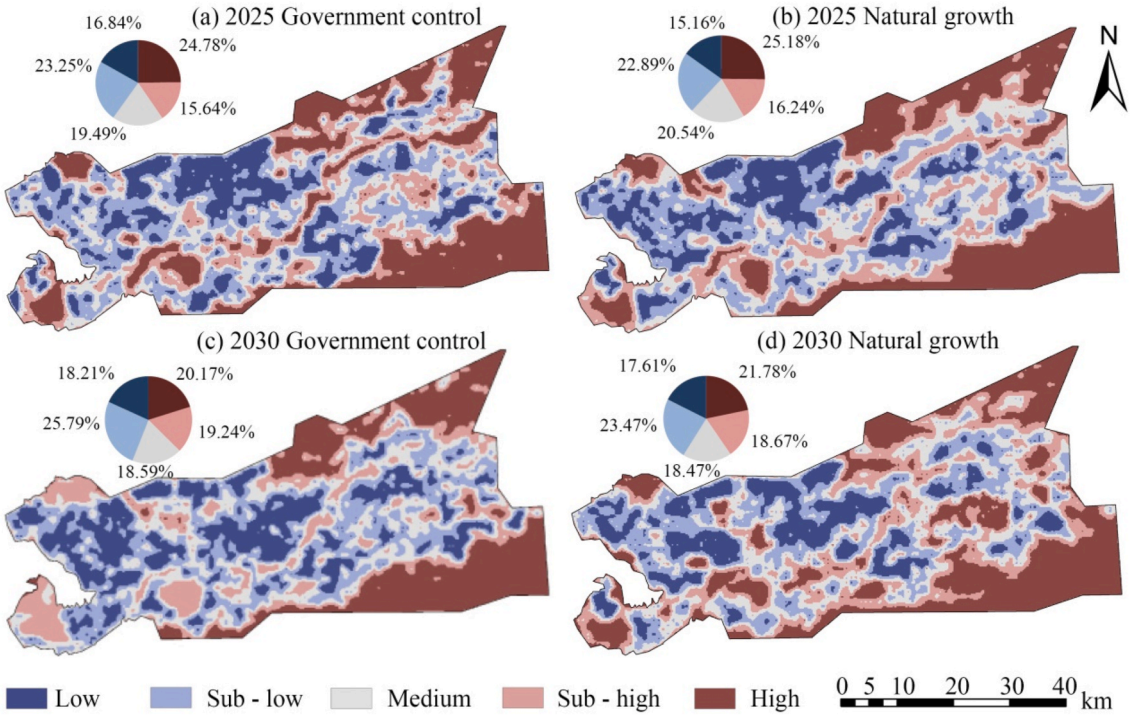

Fig. 10. Spatial patterns and proportional area of the ERI classes in 2025 and 2030 under the natural growth and government control scenarios.

(Fig. 10b); in particular, the proportion of high ecological risk areas is predicted to decrease by 0.4%, and the proportion of low ecological risk areas is predicted to increase by 1.68%. By 2030, the overall ecological risk of the study area under the government control scenario (Fig. 10c) is still predicted to be lower than the natural growth scenario (Fig. 10d) and the proportion of high ecological risk areas is predicted to decrease by 1.61%, while the proportion of low ecological risk areas is predicted to increase by 0.6%. Under the government control scenario, the government strictly controls the growth of construction and cultivated land. Thus, the area of construction and cultivated land is reduced and blind reclamation is prevented, all of which contribute to the decrease in the overall ecological risk in the study area.

From 1990 to 2019, the expansion of the cultivated land was mainly achieved through the reclamation of unused land, thereby enhancing the protection of the ecological environment and reducing the ecological risk of the study area. By 2030, as the population will continue to grow, land will continue to be reclaimed in this way to meet the demands of the human population. Thus, the ecological risk will continue to

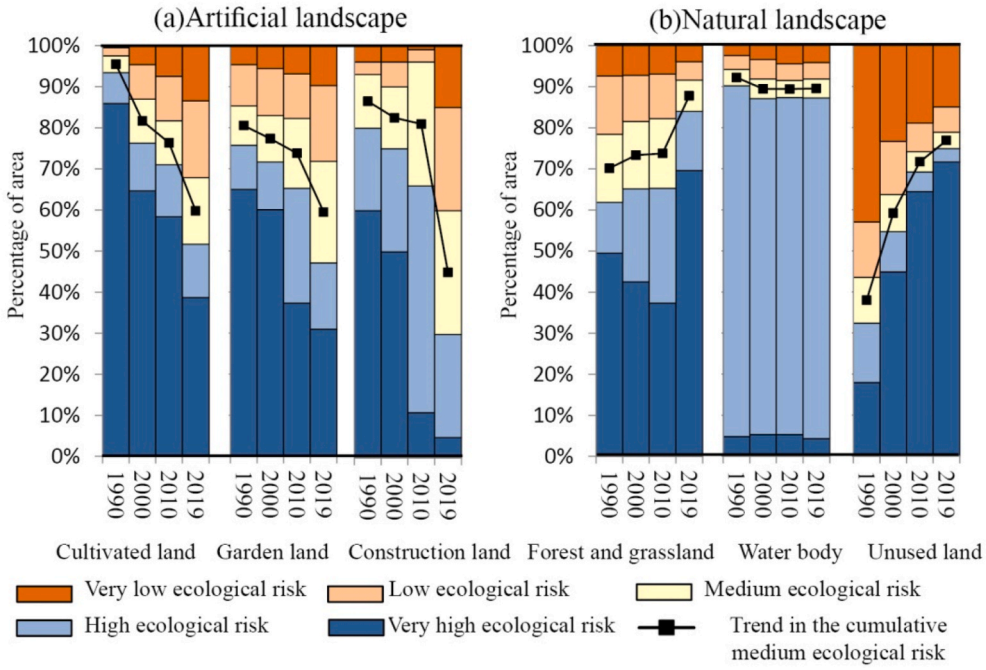

Fig. 11. The percentage change in the area of different ecological risks for different land use types from 1990 to 2019. The line graph indicates the cumulative percentage of areas less than or equal to the mean values of the medium ecological risk.

decrease. However, to prevent blind reclamation of cultivated land, the government should also introduce strict policies to control the expansion of cultivated land.

4. Discussion

4.1. Effects of land use change on ecological risks

Many researchers have confirmed that land use change is closely related to ecological risk (Xue et al., 2018, 2019). Land use change is considered one of the most important factors affecting ecosystems (Peng et al., 2014). The ecological impacts of different land use patterns and intensities have regional and cumulative characteristics, which can be directly reflected in the structure and composition of ecosystems (Wu et al., 2018). As shown in Fig. 11, regions with high ecological risk in the cultivated land, garden land, and construction land in man-made landscapes showed a decreasing trend. The annual statistics show that the population of the Alar reclamation area continued to increase during the 30 years when the ecological risk was measured (from 183,400 in 1990 to 372,100 in 2019). Therefore, larger proportions of cultivated land, garden land, and construction land are needed to meet the increasing demands of the human population. With the increasing demand for agricultural production, the originally ecologically fragile desert area became an artificial oasis area with a stable ecosystem, due to the use of more suitable technologies. This has reduced the ecological risk in these regions. In natural landscapes, areas of land with high ecological risk in forests, grasslands, and unused areas increased. The unused land is continuously reclaimed, thereby subjecting the remaining land to greater ecological risk. Usually, the unused land itself has a simple structure with low vegetation coverage, which makes the ecosystem vulnerable.

4.2. Suggestions for future policy

Due to economic development in the Alar reclamation area, the population continues to grow and the conflict between people and land is increasing. A series of exploitation problems such as the expansion of cultivated land and the continued degradation of natural forests and grasslands have been highlighted (Fu et al., 2020). Since damaged landscape ecosystems are difficult to restore (Wu et al., 2021), the pursuit of socio-economic development should not be accompanied by the neglect of ecological and environmental problems. Thus, the protection of forest land and grassland should be strengthened and blind and uncontrolled exploitation of cultivated land should be avoided. To control the blind reclamation of cultivated land, the government should strictly control the increase in the proportion of cultivated land. This is particularly important given that grasslands provide the functions of water conservation, soil conservation, greening, and landscaping, and play an important role in farming and animal husbandry in the reservoir area.

By forecasting the ecological risk in the study area under the natural growth scenario and the government control scenario, we were able to determine whether the ecological risk can be reduced under the natural growth scenario. These findings can provide important implications for implementing efficient measures and policies to restore the ecological environment and achieve sustainable development of the eco-environment. The process of converting land to construction land is almost irreversible; thus, the government should strictly control the increase in construction land when formulating the overall plan for land use. In addition, to prevent the unrestricted increase in cultivated land and to protect and improve the ecological environment in the reclamation area, the government should also strictly implement the policy of returning farmland to forest, prohibit illegal cultivation, and prevent blind reclamation of cultivated land. Moreover, the government should pay more attention to the protection of water quality.

5. Conclusion

In this study, we collected data from 259 Landsat images covering the Alar reclamation area and then used methods based on landscape ecology theory and spatial statistical analysis to construct a landscape ERI and assess the ecological risk of the Alar reclamation area. Additionally, we forecasted the ecological risk in 2025 and 2030 in the survey region. The main conclusions of this study are as follows:

(1) From 1990 to 2019, the area of cultivated land increased in the Alar reclamation area. When the degree of fragmentation decreased, the degree of dominance increased. Decrease of the areas of unused land leads to a decrease of the dominance of unused land, which indicating that the increase of external disturbances on the study area. Also, the ecological risk in the study area showed a decreasing trend, with an increase in agricultural production being the main influencing factor in the reduction of the ecological risk in the Alar reclamation area.
(2) From 1990 to 2019, the ecological risk level decreased and the areas with decreased ecological risk levels were mainly situated in the coastal area of the Tarim River and the northwestern region of the reclamation area.
(3) Compared to 2019, the ecological risk in the study area is predicted to decrease in 2025 under the scenarios of natural growth and strict government control and the proportion of high ecological risk areas is predicted to decrease by 2 and 2.4%, respectively. In 2030, the proportion of high ecological risk areas is predicted to decrease by 5.4 and 7.01% under the scenarios of natural growth and strict government control, respectively.

Compared to the natural growth scenario, the area of construction and cultivated land is predicted to reduce under the government control scenario, which can prevent the blind reclamation of cultivated land and decrease the overall ecological risk in the study area. Therefore, ecological and environmental issues cannot be ignored when pursuing social and economic development. The government should formulate a reasonable comprehensive land use plan. Furthermore, to ensure ecological balance, stricter control policies, prohibition of illegal construction activities, and prevention of blind reclamation of cultivated land are also necessary to protect forests, grasslands, and water quality.

CRediT authorship contribution statement

Qi Song: conceived and designed the research themes analysed the data. **Bifeng Hu:** contributed to revision. **Jie Peng:** conceived and designed the research themes, analysed the data. **Hocine Bourennane:** polished the paper. **Asim Biswas:** polished the paper. **Thomas Opitz:** polished the paper. **Zhou Shi:** polished the paper, All authors have contributed to the revision and approved the manuscript.

Declaration of competing interest

The authors declare that they have no known competing financial interests or personal relationships that could have appeared to influence the work that was reported in this paper.

Data availability

No data was used for the research described in the article.

Acknowledgements

This study was supported by the Young and Middle-aged Innovative Talents Program of Xinjiang Production and Construction Corps (No. 2020CB032), the National Key Research and Development Program of China (No. 2018YFE0107000), the Humanities and Social Sciences

Project of Jiangxi Education Department (GL21217), the Project of Department of Education Science and Technology of Jiangxi Province (No GJJ210541) and the Social Science Foundation of Jiangxi Province (No 21YJ43D).

References

Ama, B., Hw, A., 2020. Simulating urban land use and cover dynamics using cellular automata and Markov chain approach in addis ababa and the surrounding. Urban Clim. 31.

Cao, J., Ma, S.P., Yuan, W.H., Wu, Z.Y., 2022. Characteristics of diurnal variations of warm-season precipitation over Xinjiang Province in China. Atmos. Ocean Sci. Lett. 15 (2), 100113.

Cui, L., Zhao, Y., Liu, J., Han, L., Ao, Y., Yin, S., 2018. Landscape ecological risk assessment in Qinling Mountain. Geol. J. 53, 342–351.

Fu, J., Liu, J., Wang, X., Zhang, M., Chen, W., Chen, B., 2020. Ecological risk assessment of wetland vegetation under projected climate scenarios in the Sanjiang Plain, China. J. Environ. Manag. 273, 111108.

Ghosh, P., Mukhopadhyay, A., Chanda, A., Mondal, P., Akhand, A., Mukherjee, S., 2017. Application of cellular automata and markov-chain model in geospatial environmental modelling-a review. Remote Sensing Applications Society & Environment 5, 64–77.

He, Y., Chen, G., Potter, C., Meentemeyer, R.K., 2019. Integrating multi-sensor remote sensing and species distribution modeling to map the spread of emerging forest disease and tree mortality. Remote Sens. Environ. 231, 111238.

Hou, M., Ge, J., Gao, J., Meng, B., Li, Y., Yin, J., Liu, J., Feng, Q., Liang, T., 2020. Ecological risk assessment and impact factor Analysis of alpine wetland ecosystem based on LUCC and boosted regression tree on the Zoige plateau, China. Rem. Sens. 12 (3), 368.

Hu, B., Jia, L., Hu, J., Xu, D., Xia, F., Li, Y., 2017. Assessment of heavy metal pollution and health risks in the soil-plant-human system in the Yangtze river delta, China. Int. J. Environ. Res. Publ. Health 14 (9), 1042.

Hu, B., Shao, S., Fu, Z., Li, Y., Ni, H., Chen, S., Zhou, Y., Jin, B., Shi, Z., 2019. Identifying heavy metal pollution hot spots in soil-rice systems: a case study in South of Yangtze River Delta, China. Sci. Total Environ. 658, 614–625.

Hu, B., Shao, S., Ni, H., Fu, Z., Hu, L., Zhou, Y., Min, X., She, S., Chen, S., Huang, M., Zhou, L., Li, Y., Shi, Z., 2020a. Current status, spatial features, health risks, and potential driving factors of soil heavy metal pollution in China at province level. Environ. Pollut., 114961

Hu, B., Zhou, Y., Jiang, Y., Ji, W., Fu, Z., Shao, S., Li, S., Huang, M.X., Zhou, L.Q., Shi, Z., 2020b. Spatio-temporal variation and source changes of potentially toxic elements in soil on a typical plain of the Yangtze River Delta, China (2002–2012). J. Environ. Manag. 271, 110943.

Hu, B.F., Xie, M.D., Li, H.Y., Zhao, W.R., Hu, J., Jiang, Y.F., Ji, W.J., Li, S., Hong, Y.S., Yang, M.H., Optiz, T., Shi, Z., 2022. Stoichiometry of soil carbon, nitrogen, and phosphorus in farmland soils in Southern China: spatial pattern and related dominates. Catena 217, 106468.

Jin, X., Jin, Y.X., Mao, X.F., 2019. Ecological risk assessment of cities on the Tibetan Plateau based on land use/land cover changes–Case study of Delingha City. Ecol. Indicat. 101, 185–191.

Kabisch, N., Selsam, P., Kirsten, T., Lausch, A., Bumberger, J., 2019. A multi-sensor and multi-temporal remote sensing approach to detect land cover change dynamics in heterogeneous urban landscapes. Ecol. Indicat. 99, 273–282.

Li, F., Zhang, J., Liu, C., Xiao, M., Wu, Z., 2018. Distribution, bioavailability and probabilistic integrated ecological risk assessment of heavy metals in sediments from Honghu Lake, China. Process Saf. Environ. Protect. 116, 169–179.

Li, W., Wang, Y., Xie, S., Sun, R., Cheng, X., 2020. Impacts of landscape multifunctionality change on landscape ecological risk in a megacity, China: a case study of Beijing. Ecol. Indicat. 117, 106681.

Liang, X., Junaid, M., Wang, Z., Li, T., Xu, N., 2019. Spatiotemporal distribution, source apportionment and ecological risk assessment of PBDEs and PAHs in the Guanlan River from rapidly urbanizing areas of Shenzhen, China. Environ. Pollut. 250, 695–707.

Lv, N.N., Lu, H.Y., Pan, W., Meadows, M.E., 2022. Factors controlling spatio-temporal variations of sandy deserts during the past 110 Years in Xinjiang, Northwestern China. J. Arid Environ. 201, 104749.

Ma, L., Bo, J., Li, X., Fang, F., Cheng, W., 2019. Identifying key landscape pattern indices influencing the ecological security of inland river basin: the middle and lower reaches of Shule River Basin as an example. Sci. Total Environ. 674, 424–438.

Mokarram, M., Pourghasemi, H.R., Hu, M., Zhang, H., 2021. Determining and forecasting drought susceptibility in southwestern Iran using multi-criteria decision-making (MCDM) coupled with CA-Markov model. Sci. Total Environ. 781, 146703.

Ni, L.L., Wang, D., Singh, V.P., Wu, J.F., Wang, Y.K., Tao, Y.W., Liu, J.F., Zou, Y., He, R. M., 2019. A hybrid model-based framework for estimating ecological risk. J. Clean. Prod. 225, 1230–1240.

Ning, S.K., Chang, N.B., Jeng, K.Y., Tseng, Y.H., 2006. Soil erosion and non-point source pollution impacts assessment with the aid of multi-temporal remote sensing images. J. Environ. Manag. 79 (1), 88–101.

Peng, J., Biswas, A., Jiang, Q.S., Zhao, R.Y., Hu, B.F., Shi, Z., 2019. Estimating soil salinity from remote sensing and terrain data in Southern Xinjiang province, China. Geoderma 337, 1309–1319.

Peng, J., Hu, Y., Dong, J., Liu, Q., Liu, Y., 2020a. Quantifying spatial morphology and connectivity of urban heat islands in a megacity: a radius approach. Sci. Total Environ. 714, 136792.

Peng, J., Hu, Y., Dong, J., Mao, Q., Liu, Y., Du, Y., Wu, J., Wang, Y., 2020b. Linking spatial differentiation with sustainability management: academic contributions and research directions of physical geography in China. Prog. Phys. Geogr. 44, 14–30.

Peng, J., Liu, Y., Pan, Y., Zhao, Z., Song, Z., Wang, Y., 2014. Study on the correlation between ecological risk due to natural disaster and landscape pattern-process: review and prospect. Adv. Earth Sci. 29 (10), 1186–1196.

Rahman, M.T.U., Ferdous, J., 2021. Spatio-temporal variation and prediction of land use based on CA-Markov of southwestern coastal district of Bangladesh. Remote Sens. Appl.: Society and Environment, 100609.

Rahnama, M.R., 2020. Forecasting land-use changes in mashhad metropolitan area using cellular automata and Markov chain model for 2016-2030. Sustain. Cities Soc. 64.

Shi, C., Ding, H., Zan, Q., Li, R., 2019. Spatial variation and ecological risk assessment of heavy metals in mangrove sediments across China. Mar. Pollut. Bull. 143, 115–124.

Shi, Y.J., Xu, X.B., Li, Q.F., Zhang, M., Li, J., Lu, Y.L., Liang, R.Y., Zheng, X.Q., Shao, X. Q., 2018. Integrated regional ecological risk assessment of multiple metals in the soils: a case in the region around the Bohai Sea and the Yellow Sea. Environ. Pollut. 242, 288–297.

Sww, A., Lm, B., Wkl, B., 2020. Land use and land cover change detection and prediction in Bhutan's high altitude city of thimphu, using cellular automata and Markov chain-sciencedirect. Environmental Challenges 2.

Wang, B.B., Ding, M.J., Li, S.C., Liu, L.S., Ai, J.H., 2020a. Assessment of landscape ecological risk for a cross–border basin: a case study of the Koshi River Basin, central Himalayas. Ecol. Indicat. 117, 106621.

Wang, H., Hu, Y., Liang, Y., 2021. Simulation and spatiotemporal evolution analysis of biocapacity in Xilingol based on CA-Markov land simulation. Environ. Sustain. Indicat. 11, 100136.

Wang, J.G., Zhang, F., Jim, C.Y., Chan, N.W., Johnson, V.C., Liu, C.J., Duan, P., Bahtebay, J., 2022. Spatio-temporal variations and drivers of ecological carrying capacity in a typical mountain-oasis-desert area, Xinjiang, China. Ecol. Eng. 180, 106672.

Wang, T.Y., Wang, Z.H., Guo, L., Zhang, H.Z., Li, W.H., He, H.J., Zhong, R., Wang, D.W., Jia, D.W., Wen, Y., 2021. Experiences and challenges of agricultural development in an artificial oasis: a review. Agric. Syst. 193, 103220.

Wang, X.T., Dan, Z., Cui, X.Q., Zhang, R.X., Zhou, S.Q., Wenga, T., Yan, B.B., Chen, G.Y., Zhang, Q.Y., Zhong, L., 2020. Contamination, ecological and health risks of trace elements in soil of landfill and geothermal sites in Tibet. Sci. Total Environ. 715, 136639.

Webster, R., Oliver, M.A., 2008. Geostatistics for Environmental Scientists, second ed. Wiley, Hoboken, NJ, USA.

Wu, L., You, W., Ji, Z., Xiao, S., He, D., 2018. Ecosystem health assessment of dongshan island based on its ability to provide ecological services that regulate heavy rainfall. Ecol. Indicat. 84, 393–403.

Wu, Z., Lin, C., Shao, H., Feng, X., Chen, X., Wang, S., 2021. Ecological risk assessment and difference analysis of pit ponds under different ecological service functions-A case study of Jianghuai ecological Economic Zone. Ecol. Indicat. 129, 107860.

Xia, F., Hu, B., Shao, S., Xu, D., Zhou, Y., Zhou, Y., Shi, Z., 2019. Improvement of spatial modeling of Cr, Pb, Cd, as and Ni in soil based on portable X-ray fluorescence (PXRF) and geostatistics: a case study in east China. Int. J. Environ. Res. Publ. Health 16 (15), 2694.

Xia, F., Hu, B., Zhu, Y., Ji, W., Chen, S., Xu, D., Shi, Z., 2020. Improved mapping of potentially toxic elements in soil via integration of multiple data sources and various geostatistical methods. Rem. Sens. 12 (22), 3775.

Xie, H.L., He, Y.F., Choi, Y., Chen, Q.R., Cheng, H., 2020. Warning of negative effects of land-use changes on ecological security based on GIS. Sci. Total Environ. 704, 135427.

Xu, J., Kang, J., 2017. Comparison of ecological risk among different urban patterns based on system dynamics modeling of urban development. J. Urban Plann. Dev. 143 (2), 04016034.

Xu, T., Weng, B.S., Yan, D.H., Wang, K., Li, X.N., Bi, W.X., Li, M., Cheng, X.J., Liu, Y.X., 2019. Wetlands of international importance: status, threats, and future protection. Int. J. Environ. Res. Publ. Health 16 (10), 1818.

Xue, L., Yang, F., Yang, C., Wei, G., Li, W., He, X., 2018. Hydrological simulation and uncertainty analysis using the improved TOPMODEL in the arid Manas River basin, China. Sci. Rep. 8 (1), 1–12.

Xue, L.Q., Zhu, B.L., Wu, Y.P., Wei, G.H., Liao, S.M., Yang, C.B., Wang, J., Zhang, H., Ren, L., Han, Q., 2019. Dynamic projection of ecological risk in the Manas River basin based on terrain gradients. Sci. Total Environ. 653, 283–293.

Yu, G., Feng, J., Che, Y., Lin, X., Hu, L., Yang, S., 2010. The identification and assessment of ecological risks for land consolidation based on the anticipation of ecosystem stabilization: a case study in Hubei Province, China. Land Use Pol. 27 (2), 293–303.

Yuan, Y., Fang, G., Yan, M., Sui, C., Ding, Z., Lu, C., 2019. Flood-landscape ecological risk assessment under the background of urbanization. Water 11 (7), 1418.

Zhang, W., Chang, W.J., Zhu, Z.C., Hui, Z., 2020. Landscape ecological risk assessment of Chinese coastal cities based on land use change. Appl. Geogr. 117, 102174.

Zhang, R.Q., Li, P.H., Xu, L.P., Zhong, S., Wei, H., 2022. An integrated accounting system of quantity, quality and value for assessing cultivated land resource assets: a case study in Xinjiang, China. Global. Ecol. Conserv. 36, e02115.

Zhang, Y., Chang, X., Liu, Y., Lu, Y., Wang, Y., Liu, Y., 2021a. Urban expansion simulation under constraint of multiple ecosystem services (MESs) based on cellular automata (CA)-Markov model: scenario analysis and policy implications. Land Use Pol. 108, 105667.

Zhang, Y., Zhang, F., Zhou, M., Li, X.H., Ren, Y., Wang, J., 2016. Landscape ecological risk assessment and its spatio-temporal variations in Ebinur Lake region of inland arid area. Yingyong Shengtai Xuebao 27 (1).
Zhang, Z., Hu, B., Jiang, W., Qiu, H., 2021b. Identification and scenario prediction of degree of wetland damage in Guangxi based on the CA-Markov model. Ecol. Indicat. 127, 107764.
Zheng, Y., Yang, Q.Y., Ren, H., Wang, D.J., Zhao, C.M., Zhao, W.Z., 2022. Spatial pattern variation of artificial sand-binding vegetation based on UAV imagery and its influencing factors in an oasis–desert transitional zone. Ecol. Indicat. 141, 109068.